Journal of the Optical Society of America B
OPTICAL PHYSICS

Compensation method for temperature-induced phase mismatch during frequency conversion in high-power laser systems

Zijian Cui,[1,2] Dean Liu,[1,*] Meizhi Sun,[1] Jie Miao,[1] and Jianqiang Zhu[1]

[1]Shanghai Institute of Optics and Fine Mechanics, Chinese Academy of Sciences, Shanghai 201800, China
[2]University of Chinese Academy of Sciences, Beijing 100049, China
*Corresponding author: liudean@siom.ac.cn

Received 2 December 2015; revised 27 January 2016; accepted 28 January 2016; posted 1 February 2016 (Doc. ID 254906); published 8 March 2016

A compensation method for phase mismatch caused by temperature variation during the frequency conversion process is proposed and the theoretical model is established. The method is based on the principle that phase mismatch can be compensated via the electro-optic effect based on a compensation scheme consisting of two nonlinear crystals and an electro-optic crystal; further, a new dimension adjustment can be achieved by changing the voltage. In a proof-of-principle study, frequency conversion from 1053 nm to 526.5 nm and 351 nm by cascade KH_2PO_4 (KDP) and KD_2PO_4 (DKDP) crystals, respectively, is presented as an example. Three-dimensional numerical simulations are conducted to show that the conversion efficiency of frequency doubling and tripling varies with temperature. The results show that the temperature acceptance bandwidth of doubling and tripling can be 2.4 and 3.4 times larger, respectively, than that of the traditional method using a single crystal. We also analyze the stability of the conversion efficiency for 192 beams by our proposed method when the temperature is randomly varied within the range of 24°C–26°C. The standard deviation of the conversion efficiency of frequency doubling and tripling decreases from 1.25% and 6.61% to 0.18% and 0.56%, respectively. In addition, the influence of the reflection loss on the output efficiencies is also analyzed and the results show that it is very small. This indicates that this method may be effective in reducing the temperature sensitivity of conversion efficiency.

OCIS codes: (140.3515) Lasers, frequency doubled; (190.2620) Harmonic generation and mixing; (190.4223) Nonlinear wave mixing.

http://dx.doi.org/10.1364/JOSAB.33.000525

1. INTRODUCTION

Frequency conversion is an important method to extend the working wavelength of various laser sources using nonlinear crystals (e.g., BaB_2O_4 (BBO), LiB_3O_5 (LBO), KH_2PO_4 (KDP), KD_2PO_4 (DKDP), and $KTiOPO_4$ (KTP) [1]) and to enable the use of Nd:glass laser systems as short-wavelength lasers for inertial confinement fusion (ICF). A typical system is the National Ignition Facility (NIF), which contains 192 laser beams. The total energy of its third-harmonic pulses (351 nm) can reach 1.8 MJ with a peak power of 500 TW [2,3]. During the frequency conversion process, it is difficult to control temperature with high precision for large laser systems. Since the refractive index of nonlinear crystals is dependent on temperature, the problem of phase mismatch will arise when the temperature deviates from the perfect phase-matching temperature, resulting in a decrease in conversion efficiency [4,5]. Frequency conversion is an essential method for ultrashort ultraviolet pulse generation and plays a key role in the laser inertial confinement fusion systems [6,7]. The stability of the conversion efficiency is very important, particularly for large high-power laser systems such as the NIF. The NIF is able to obtain precisely specified powers from each of the 192 beams over a wide variety of pulse lengths and temporal shapes, and is able to minimize the deviation in the distribution of energy and power between beams with very high precision (<3% and <8% beam to beam, respectively) [7]. These are essential for success on a number of the NIF lasers' missions. Consequently, the balance of energy and power among the beams has high requirements for temperature control precision and stability. However, it is a challenge for large laser systems to meet these requirements.

In order to minimize the effect of temperature on conversion efficiency in the frequency conversion process, several cooling configurations and temperature control schemes have been proposed to control the crystal temperature, including

beam shaping, gas-cooled multiple-plate designs, and temperature-insensitive phase-matching scheme designs [8–11]. However, these techniques require extremely sophisticated components or are limited in their scopes of application. For instance, the temperature-insensitive phase-matching scheme design requires two different crystals that have opposite signs of the first derivation of phase mismatch with respect to temperature ($\partial\Delta k/\partial T$) at a specific fundamental wavelength [11,12]. Currently, commonly used nonlinear crystals such as KDP, DKDP and BBO have a positive first derivative ($\partial\Delta k/\partial T > 0$) and, as of now, $YCa_4O(BO_3)_3$ (YCOB) and LBO crystals have a negative first derivative ($\partial\Delta k/\partial T < 0$) at near infrared [12]. At present, the maximum clear aperture of a YCOB crystal is 60–70 mm [13]. The maximum clear aperture of a LBO crystal is 150 mm, but they are difficult to grow and are costly due to the long growth time [14]. Therefore, this method is not applicable in cases where large aperture crystals are needed, such as in the ICF experiment (the KDP crystals have a square clear aperture of ~310 mm and ~400 mm in SG II (a high power laser facility in Shanghai Institute of Optics and Fine Mechanics) and NIF, respectively [3,7]). In addition, these methods are mainly applied to solve the temperature changes of the single beam. For large laser systems with many beams (e.g., NIF), the balance of efficiency among multibeams is very important. We mainly aim at reducing the influence of the temperature difference among the multibeams on the balance of efficiency in the large laser systems.

Here, we propose a novel scheme to compensate for the phase mismatch in the frequency conversion process of a high-power laser. There are two nonlinear crystals and an electro-optic crystal in tandem and the electro-optic crystal is placed between two nonlinear crystals. The tunable phase mismatch compensation can be achieved by changing the voltage. Unlike the previous temperature-insensitive design, it does not require the optimization of the lengths of two crystals based on the incident light intensity and $\partial\Delta k/\partial T$. The phase mismatch compensation scheme is shown in Fig. 1.

In the process of frequency conversion, the laser beams pass through the first nonlinear crystal, the electro-optic crystal, and the second nonlinear crystal in this order. The phase mismatch caused by temperature variation in the first nonlinear crystal is compensated effectively by the electro-optic effect of the electro-optic crystal. Thus, frequency conversion with high efficiency can be achieved in a wide temperature range.

The phase mismatch value (PMV) of the beams arising from the first nonlinear crystal can be calculated using the temperature deviation and the length of the first nonlinear crystal. In order to compensate for the phase mismatch as the beams pass through the electro-optic crystal, the appropriate polarization directions of the laser beams and the voltage of the load in the electro-optic crystal should be selected. The size of this voltage can be determined from the PMV, the polarization directions of the beams, and the length and height of the electro-optic crystal. Different voltage values for different temperatures can be calculated. When the temperature is changed, the corresponding voltage value can be selected to compensate for the phase mismatch and a high-efficiency frequency conversion in a wide temperature range can be realized.

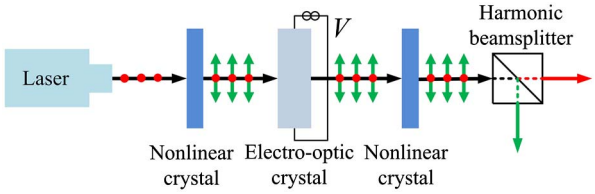

Fig. 1. Phase mismatch compensation scheme.

As mentioned previously, this paper mainly discusses the solution to the influence of the temperature difference among the multibeams on the balance of efficiency in the laser fusion systems. Since laser fusion systems operate at a very low repetition rate, the temperature of each crystal can be regarded as uniform. This method is suitable for the situation that temperature changes uniformly.

2. THEORETICAL MODEL OF PHASE MISMATCH COMPENSATION

The electro-optic modulation of light waves can be divided into transverse electro-optic modulation and longitudinal electro-optic modulation, according to the direction of the applied electric field [15]. Since the direction of the electric field in longitudinal electro-optic modulation is consistent with the propagation direction of the beams, a transparent electrode is required; however, this will also reduce the quality of the laser beam. Therefore, we will use transverse electro-optic modulation.

Owing to their favorable optical properties and high optical uniformity, KDP and its isomorph DKDP are the materials of choice for frequency conversion and electro-optical switching in high-power laser systems [16,17]. Compared with KDP, DKDP has a larger electro-optic coefficient (the electro-optic coefficients of KDP and DKDP are $r_{63} = -10.3$ pm/V and $r_{63} = -25.8$ pm/V [18], respectively). Therefore, the required voltage of DKDP is much smaller than that of KDP. Therefore, DKDP is used as an electro-optic crystal.

According to the refractive index ellipsoid of a uniaxial crystal, the new principal axes x' and y' are rotated by 45° from the original x and y axes around the z axis (the optical axis) when an electric field is applied to DKDP along the z direction. The rotation angle is independent of the size of the applied electric field. If $n_o^2\gamma_{63}E_z \ll 1$, which is true for any reasonable electric field, the DKDP crystal will become biaxial and the new principal refractive indices are given by [19]

$$n_{x'} = n_o - \frac{1}{2}n_o^3\gamma_{63}E_z, \tag{1a}$$

$$n_{y'} = n_o + \frac{1}{2}n_o^3\gamma_{63}E_z, \tag{1b}$$

$$n_{z'} = n_e, \tag{1c}$$

where n_o and n_e are the ordinary and extraordinary refractive indices, respectively; γ_{63} is the electro-optic coefficient; E_z is the electric field intensity (given by $E_z = V/d$); V is the voltage applied to the electro-optic crystal; d is the distance between the two electrodes; and $n_{x'}$, $n_{y'}$ and $n_{z'}$ are the new

principal refractive indices in the presence of an external electric field applied parallel to the z axis of electro-optic crystal.

Let the lengths of the two nonlinear crystals be L_1 and L_2, respectively, the perfect phase-matching temperature be T_0, and the phase-matching angle be θ_m. The length of the electro-optic crystal is L, and the height is d (i.e., the distance between the two electrodes). The refractive indices of the laser beams in the first nonlinear crystal can be calculated by the Sellmeier equation [20], and the corresponding phase mismatch can be obtained using the refractive indices and wavelengths,

$$\frac{1}{n_e^2(\theta_m, T)} = \frac{\cos^2\theta_m}{n_o^2(T)} + \frac{\sin^2\theta_m}{n_e^2(T)}, \tag{2a}$$

$$\Delta k_1 = \frac{2\pi}{\lambda_3} n_3(T, \theta_m, \lambda_3) - \frac{2\pi}{\lambda_2} n_2(T, \theta_m, \lambda_2) - \frac{2\pi}{\lambda_1} n_1(T, \theta_m, \lambda_1), \tag{2b}$$

where λ_i and n_i $(i = 1, 2, 3)$ are the corresponding wavelengths and refractive indices of the beams, respectively; Δk_1 is the phase mismatch of the beams in the first nonlinear crystal.

From the phase mismatch, the PMV of the output beams from the first nonlinear crystal can be obtained:

$$\Delta K_1 = \Delta k_1 \cdot L_1. \tag{3}$$

The refractive indices n_i' $(i = 1, 2, 3)$ can be calculated from Eq. (1) when the beams propagate in the electro-optic crystal. The phase mismatch of the beams in the electro-optic crystal is

$$\Delta k = \frac{2\pi}{\lambda_3} n_3' - \frac{2\pi}{\lambda_2} n_2' - \frac{2\pi}{\lambda_1} n_1'. \tag{4}$$

In order to achieve high-efficiency frequency conversion, ΔK_1 needs to be compensated, and thus the PMV of beams emitted from the electro-optic crystal should satisfy the following condition [10],

$$\Delta K = \Delta K_1 + \Delta k \cdot L = N \cdot 2\pi, \tag{5}$$

where N is an integer. If the temperature changes, the corresponding electric field intensity and voltage value can be obtained by Eqs. (1)–(5).

In order to compensate for the phase mismatch arising in the first nonlinear crystal at different temperatures, the variation range of PMV should be 2π in the electro-optic crystal. Since the PMV for the beams emitted from the first nonlinear crystal will fall over different ranges at different temperatures, it should be adjusted to a suitable integer multiple of 2π after the beams pass through the electro-optic crystal. This can be determined according to the following equation:

$$\Delta K = |\Delta K_1 + \Delta k \cdot L| = \begin{cases} N \cdot 2\pi & \text{if } (2N+1)\pi \geq |\Delta K_1| \geq N \cdot 2\pi \\ (N+1) \cdot 2\pi & \text{if } (N+1) \cdot 2\pi \geq |\Delta K_1| \geq (2N+1)\pi \end{cases}. \tag{6}$$

The schematic diagram in Fig. 2 shows the change in PMV of the beams during transmission.

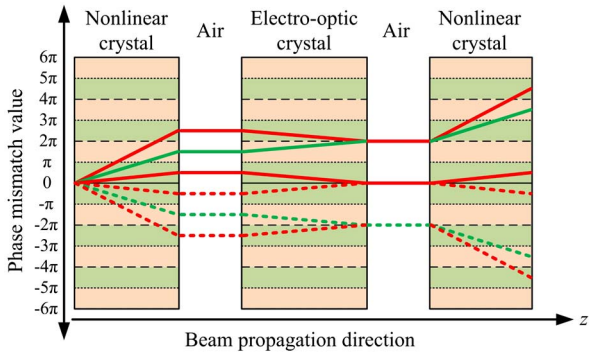

Fig. 2. Schematic diagram of PMV change when the beams are emitted from the first nonlinear crystal. Crystal temperature above T_0 is represented by a solid line; crystal temperature below T_0 is represented by a dashed line. The red lines show where the absolute value of PMV falls within $(2n+1)\pi \geq |\Delta K_1| \geq 2n\pi$; the green lines show where the absolute value of PMV falls within $(2n+2)\pi \geq |\Delta K_1| \geq (2n+1)\pi$. For red and green lines, the PMV will be compensated to $2n\pi$ and $(2n+2)\pi$ in the electro-optic crystal, respectively.

As described above, the method only needs to satisfy the condition that the wavelengths of the beams falling in the transmission region of the electro-optic crystal and the phase mismatch value vary over a range of 2π. The phase mismatch can be well compensated by the electro-optic effect at different temperatures. Therefore, this method is almost completely independent of nonlinear crystal type and beam wavelengths, and can be applied to both type-I and type-II frequency conversion for different nonlinear crystals.

3. NUMERICAL SIMULATIONS AND RESULTS ANALYSIS

In this section, we theoretically studied the phase mismatch compensation scheme in the case of the KDP crystal for frequency doubling with type-I and tripling with type-II. We take Nd:glass laser (1053 nm) as the incident fundamental wave with a pulse duration of 1 ns and a maximum intensity up to 1.0 GW/cm^2. Both temporal waveform and spatial distribution of the fundamental wave are six-order super-Gaussian. Laser spot is a square with a length of 10 mm. The initial perfect phase-matching temperature for the KDP crystals is 25°C (i.e., $T_0 = 25$°C), and the temperature is adjusted over the range of 15°C–35°C.

A. Basic Equations for Calculations

As we focused on the frequency conversion for nanosecond-level high-power nonchirped laser pulses or quasi-continuous lasers, the time effects (such as group-velocity mismatch, group-velocity dispersion, etc.) can be neglected [21,22]. According to the slowly varying envelope and plane-wave approximation and considering diffraction, walk-off effects and ignoring the transmission loss of beams, the nonlinear coupled-wave equations of the frequency doubling with type-I are [22–24]

$$\frac{\partial A_1}{\partial z} \cong \frac{i}{2k_{1o}}\nabla_\perp^2 A_1 + \frac{i\omega_1}{n_{1o}c} d_{\text{eff}} A_1^* A_2 \exp[i\Delta k_{\text{I}}(T)z], \tag{7a}$$

$$\frac{\partial A_2}{\partial z} \cong \frac{i}{2k_{2e}}\nabla_\perp^2 A_2 + \frac{i\omega_2}{2n_{2e}c} d_{\text{eff}} A_1 A_1 \exp[-i\Delta k_{\text{I}}(T)z] - \rho_{2e}(\theta)\frac{\partial A_2}{\partial y}. \tag{7b}$$

Similar equations for frequency tripling with type-II can be written as

$$\frac{\partial A_1}{\partial z} \cong \frac{i}{2k_{1e}}\nabla_\perp^2 A_1 + \frac{i\omega_1}{n_{1e}c} d_{\text{eff}} A_2^* A_3 \exp[i\Delta k_{\text{II}}(T)z] - \rho_{1e}(\theta)\frac{\partial A_1}{\partial y}, \tag{8a}$$

$$\frac{\partial A_2}{\partial z} \cong \frac{i}{2k_{2o}}\nabla_\perp^2 A_2 + \frac{i\omega_2}{n_{2o}c} d_{\text{eff}} A_1^* A_3 \exp[i\Delta k_{\text{II}}(T)z], \tag{8b}$$

$$\frac{\partial A_3}{\partial z} \cong \frac{i}{2k_{3e}}\nabla_\perp^2 A_3 + \frac{i\omega_3}{n_{3e}c} d_{\text{eff}} A_1 A_2 \exp[-i\Delta k_{\text{II}}(T)z] - \rho_{3e}(\theta)\frac{\partial A_3}{\partial y}, \tag{8c}$$

where the subscripts 1, 2, 3, o, and e represent the fundamental wave, second harmonic, third harmonic, ordinary field, and extraordinary field, respectively; A_i is the complex amplitude of optical field; ω_i is angular frequency; n_{ij} and k_{ij} are the refractive index and wave vector in nonlinear crystal, respectively; $\rho_{ij}(\theta)$ is the tangent of the angle between the wave normal and the Poynting vector for an extraordinary wave, where $i = 1, 2, 3$, $j = o, e$; and c and z represent the velocity of light in vacuum and the propagation distance of beams, respectively; $\nabla_\perp = \partial^2/\partial x^2 + \partial^2/\partial y^2$, where x and y are the transverse Cartesian coordinates along the nonsensitive and sensitive directions of the crystal in the plane orthogonal to the z direction of propagation, respectively; d_{eff} is the effective nonlinear coefficient; $\Delta k_{\text{I}}(T)$ and $\Delta k_{\text{II}}(T)$ are the phase mismatches of doubling and tripling given by $\Delta k_{\text{I}}(T) = k_{2e} - 2k_{1o}$ and $\Delta k_{\text{II}}(T) = k_{3e} - k_{2o} - k_{1e}$, respectively. In the coupled-wave equations [i.e., Eqs. (7) and (8)], the fundamental wave is narrowband.

For KDP crystals, type-I phase-matching frequency doubling allows an extraordinary beam of frequency $\omega_2 = 2\omega_1$ to be generated from the incident ordinary beam of frequency ω_1. Type-II frequency tripling generates an extraordinary beam of frequency $\omega_3 = \omega_1 + \omega_2$ from one ordinary beam with frequency ω_2 and one extraordinary beam with frequency ω_1. If the temperature of the crystals is T, the phase mismatch Δk_{I} and Δk_{II} (which arise from the frequency doubling and tripling crystals, respectively) can be calculated as follows:

$$\Delta k_{\text{I}} = \frac{2\pi}{\lambda_2} n_{2e}(T, \theta_m, \lambda_2) - 2\frac{2\pi}{\lambda_1} n_{1o}(T, \lambda_1), \tag{9a}$$

$$\Delta k_{\text{II}} = \frac{2\pi}{\lambda_3} n_{3e}(T, \theta_m, \lambda_3) - \frac{2\pi}{\lambda_2} n_{2o}(T, \lambda_2) - \frac{2\pi}{\lambda_1} n_{1e}(T, \theta_m, \lambda_1). \tag{9b}$$

The polarization directions of the beams in the phase-mismatch compensation scheme by KDP and DKDP crystals for frequency doubling and tripling are shown in Fig. 3.

The electro-optic crystal is used to compensate for the phase mismatch, and the transverse electro-optic modulation is used. The direction of the electric field is always along the z axis of DKDP crystal [Figs. 3(a) and 3(b)], and the directions of the beams propagation are always in the $x' - y'$ plane. In order to avoid the walk-off effect in the electro-optic crystal, the directions of beams propagation should be along the principal optic axis [15,25]. We set the directions of the beams propagation along the y' and x' axis of the DKDP crystal for frequency doubling and tripling, respectively [Figs. 3(a) and 3(b)]. Therefore, the walk-off effect in the electro-optic crystal does not exist and the output efficiency will not be affected.

We calculated the first derivations of phase mismatch with respect to the temperature of frequency doubling and tripling by KDP crystals at the fundamental wave of 1053 nm to give $\partial\Delta k_{\text{I}}/\partial T = 0.537/(\text{cm} \cdot ^\circ\text{C})$ and $\partial\Delta k_{\text{II}}/\partial T = 0.935/(\text{cm} \cdot ^\circ\text{C})$, respectively. It can be seen that frequency tripling is more sensitive to temperature than doubling and we can predict that the temperature acceptance bandwidth of frequency tripling is smaller than that of doubling.

At high intensity, the refractive index of the crystals will change with the light intensity, primarily because of the third-order nonlinear susceptibility. This will result in nonlinear phase modulation [26–28]. The relation between the refractive index of the crystals and the light intensity is given by [27]

$$n = n_0 + \Delta n = n_0 + \gamma I, \tag{10}$$

where n_0 represents the refractive index at low intensity and Δn is the nonlinear refractive index; γ is the nonlinear refractive index coefficient; and I is the light intensity. For KDP and DKDP, the variation range of γ is $2\text{–}4 \times 10^{-7}$ cm^2/GW in the wavelength range of 1064–400 nm [27,28], and the variation range of Δn is $2\text{–}4 \times 10^{-7}$ at a power density of

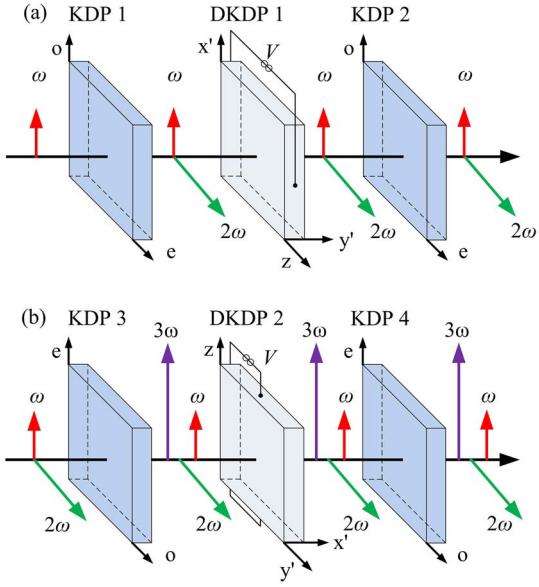

Fig. 3. Polarization directions of beams. (a) Type-I frequency doubling. (b) Type-II frequency tripling.

1 GW/cm^2. It can be evaluated that the nonlinear phase modulation-induced frequency doubling and tripling phase mismatch are about 0.0119/cm and 0.0239/cm, respectively, which are far less than temperature-induced phase mismatch [0.537/(cm · °C) and 0.935/(cm · °C)]. Therefore, at a power density of 1 GW/cm^2 with the pulse width of 1 ns, the effect of nonlinear phase modulation on frequency conversion efficiency is very small. In the nonlinear coupled-wave equations, higher-order nonlinear effects (e.g., nonlinear phase modulation) are neglected, and the temperature variation is considered by taking into account a temperature-induced $\Delta k(T)$. The nonlinear coupled-wave equations are solved using the split-step Fourier transform approach and the fourth-order Runge–Kutta algorithm [23,24]. The parameters used in the simulation are adopted directly from or calculated on the basis of the data in [18,20]. Next, we will numerically calculate the temperature acceptance bandwidths of frequency doubling and tripling.

B. Results for Frequency Doubling and Tripling

For frequency tripling, the frequencies ω_i satisfy the relationship $\omega_3 = \omega_1 + \omega_2$, the photon number of the fundamental wave (ω_1) and doubling (ω_2) matching is an important constraint for frequency tripling the conversion efficiency (theoretically, the optimum ratio of photon number and energy of the fundamental wave and doubling are 1∶1 and 1∶2, respectively), and thus the frequency doubling conversion efficiency should not be too high. The frequency doubling and tripling efficiencies are defined by $\eta_2 = E(\omega_2)/E(\omega_1)$ and $\eta_3 = E(\omega_3)/E(\omega_1)$, respectively. Here, $E(\omega_1)$ is the initial energy of the fundamental wave; $E(\omega_2)$ is the energy of frequency doubling emitted from the KDP 2 [as shown in Fig. 3(a)]; and $E(\omega_3)$ is the energy of frequency tripling emitted from the KDP 4 [as shown in Fig. 3(b)]. In order to obtain high-frequency tripling conversion efficiency, the lengths of KDP crystals should be suitable; the optimal lengths of crystals can be approximately determined by numerical calculations based on the coupled-wave equations [i.e., Eqs. (7) and (8)]. In this paper, the lengths of each KDP crystal for frequency doubling and tripling are 8.0 mm and 7.0 mm, respectively. The general high-voltage pulse generator used for electro-optic modulation can generate ten thousand volts or more [29,30]. Therefore, the voltage variation range is assumed at 0–10 kV. In order to satisfy the conditions of the electro-optic crystal described in the second section, we calculated the required size of the electro-optical crystal. Both the width and height of the electro-optical crystal are 15 mm and the length of the electro-optical crystal is 20 mm; the electro-optic coefficient is $r_{63} = -25.8$ pm/V. The maximum change of frequency doubling and tripling PMV in the electro-optic crystal can reach 6.83 and 7.05 (change range more than 2π), respectively.

First, the type-I frequency doubling process for the Nd:glass laser was studied within a temperature variation range of 15°C–35°C (Fig. 4). In the simulations, we altered the temperature of the KDP crystals over the variation range in increments of 0.5°C.

Figure 4 shows the frequency doubling conversion efficiency variation with temperature after the beams pass through the second KDP crystal under the high-power regime with a fundamental wave intensity of 1.0 GW/cm^2. A maximum conversion efficiency of 53.6% is obtained when the doubling crystals are operated at the initial perfect phase-matching temperature ($T = 25$°C and $\Delta k = 0$). If the phase mismatch caused by temperature variation is not compensated (in which the structure can be regarded as a single crystal), the conversion efficiency will rapidly decline, as shown by line A. The temperature acceptance bandwidth is 5.9°C as defined by the full width at half-maximum (FWHM), and is quite sensitive to temperature variation. If phase mismatch is compensated by our proposed method, the temperature acceptance bandwidth is as much as 2.4 times larger than that of using a single crystal, and the temperature acceptance bandwidth is increased to 14.4°C.

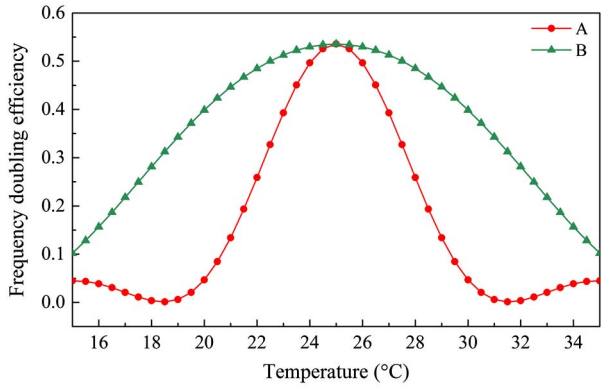

Fig. 4. Calculated conversion efficiency of type-I frequency doubling by two 8 mm long KDP crystals with respect to temperature. The circle symbol (line A) indicates phase mismatch without compensation; the triangle symbol (line B) indicates that the phase mismatch is compensated.

As the frequency tripling process is based on doubling, the frequency doubling conversion efficiency will have an effect on the tripling conversion efficiency. Therefore, the frequency tripling conversion efficiency is not only related to the tripling crystal temperature, but also to the frequency doubling conversion efficiency. In fact, both the doubling and tripling temperatures can be changed, and thus the influence of the frequency doubling process on the temperature acceptance bandwidth of tripling should be taken into account. Four combinations of the phase mismatch compensation scheme for tripling are listed in Table 1. We analyzed the temperature-dependent conversion efficiency and temperature acceptance bandwidth of tripling with respect to the above-mentioned conditions, and the results are shown in Fig. 5.

Table 1. Phase Mismatch Compensation Combinations for Tripling

	Frequency Doubling	Frequency Tripling
A	No	No
B	No	Yes
C	Yes	No
D	Yes	Yes

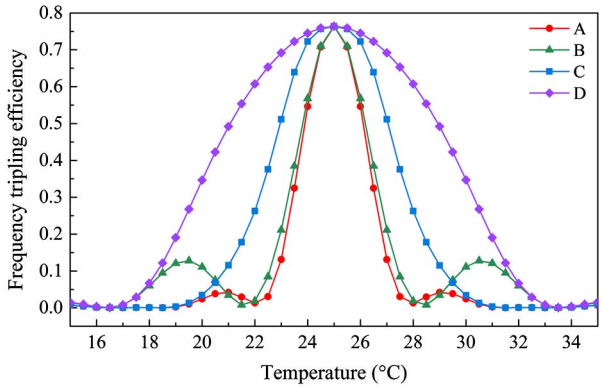

Fig. 5. Calculated conversion efficiency of type-II frequency tripling by two 7 mm long KDP crystals based on doubling with respect to temperature. The circle symbol (line A) indicates both the doubling and tripling phase mismatch without compensation; the triangle symbol (line B) indicates that only the doubling phase mismatch is compensated; the square symbol (line C) indicates that only the tripling phase mismatch is compensated; the diamond symbol (line D) indicates that both the doubling and tripling phase mismatch are compensated.

According to line A in Fig. 5, the temperature acceptance bandwidth of frequency tripling is 2.8°C. A maximum conversion efficiency of 76.4% is obtained when the doubling and tripling crystals are operated at the initial perfect phase-matching temperature. Comparing line A in Fig. 4 with that in Fig. 5, we can see that the frequency tripling conversion efficiency is more sensitive to temperature variation than that of the frequency doubling, which is consistent with $\partial\Delta k_{\mathrm{I}}/\partial T < \partial\Delta k_{\mathrm{II}}/\partial T$. From line A and line B in Fig. 5, it can be seen that the temperature acceptance bandwidth of line B (3.0°C) is only slightly larger than that of line A. The reason is that the phase mismatch is compensated only in the frequency doubling process for line B. This enhances the stability of the doubling conversion efficiency, but the sensitivity of the tripling conversion efficiency to temperature is not reduced. Consequently, the change of line B relative to line A is very small. Although the temperature acceptance bandwidth is increased slightly, this is because the stability of the frequency doubling conversion efficiency is improved. Comparing line A and line C in Fig. 5, the temperature acceptance bandwidth of line C is increased to 1.8 times (4.9°C) despite the fact that the frequency doubling phase mismatch is not compensated. The temperature acceptance bandwidth of frequency tripling can be effectively increased. This is because the frequency tripling conversion efficiency is more sensitive to temperature variation. When the temperature is changed, the rate of decrease of the frequency doubling conversion efficiency is slower than that of tripling. Therefore, compensating the phase mismatch in the frequency tripling process is more effective than doing so in the frequency doubling process in improving the temperature acceptance bandwidth of frequency tripling.

We can conclude that the phase mismatch compensation for the frequency doubling process has little effect in increasing the temperature acceptance bandwidth of tripling. To increase the acceptance bandwidth of frequency tripling, the phase mismatch compensation for tripling is more effective than doubling, as shown by comparing line B and line C. If the phase mismatches of frequency doubling and tripling are compensated, the temperature acceptance bandwidth of frequency tripling would be as high as 9.5° C (line D), which is 3.4 and 1.9 times larger than that of the traditional method (line A, 2.8°C) and tripling phase mismatch with compensation (line C, 4.9°C), respectively. Comparing line C and line D in Fig. 5, we can find that phase mismatch compensation for frequency doubling has an obvious effect on the increase of the temperature acceptance bandwidth of tripling when the tripling phase mismatch is compensated. This is because the temperature acceptance bandwidth of frequency tripling with phase mismatch compensation (line C in Fig. 5, 4.9°C) is close to that of the frequency doubling without phase mismatch compensation (line A in Fig. 4, 5.9°C). It is only in this case that the stability of the frequency doubling conversion efficiency will significantly increase the temperature acceptance bandwidth of tripling.

The required voltages at different temperatures are shown in Fig. 6. The temperature is altered in increments of 0.5°C.

Since the efficiency of the frequency tripling is more sensitive to temperature than that of doubling, the variation of voltage for the frequency tripling phase mismatch compensation (~1.8 kV) is larger than that for frequency doubling (~1.5 kV) each time. However, the maximum voltage required for frequency tripling phase mismatch compensation (~8.0 kV) is smaller than that for frequency doubling (~9.0 kV). This is because the maximum change of frequency tripling PMV (7.05) in the DKDP crystal is larger than that of doubling PMV (6.83). In fact, the phase mismatch can be well compensated as long as the maximum change of PMV reaches 2π.

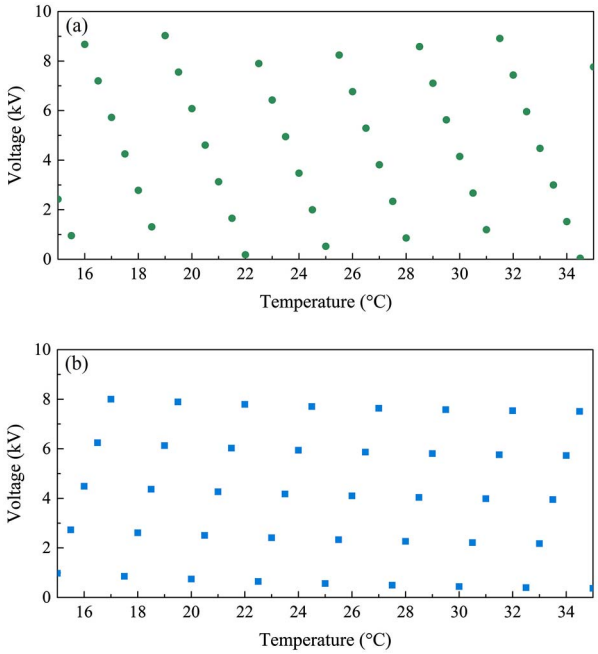

Fig. 6. Calculated phase mismatch compensation voltage versus the crystal temperature. (a) Type-I frequency doubling. (b) Type-II frequency tripling.

C. Evolutions of Conversion Efficiency in the Crystal with Temperature Shift

For frequency doubling and tripling by the traditional method with a single crystal, the conversion efficiencies are decreased by approximately 50% and 100%, respectively, when the temperature deviates from the perfect phase-matching temperature of ±3°C (as shown by line A in Fig. 4 and in Fig. 5). In order to clearly present the evolutions of the conversion efficiency in the crystals under different situations, we compared and analyzed the relationship between the conversion efficiency and transmission distance in the KDP crystals for frequency doubling and tripling at temperature offset of 3°C. The conversion efficiency variation of frequency doubling and tripling in the cascade of KDP crystals (where each KDP crystal length is 8.0 mm with a total length of 16.0 mm for doubling crystals, and 7.0 mm with a total length of 14.0 mm for tripling crystals) are shown in Figs. 7(a) and 7(b), respectively.

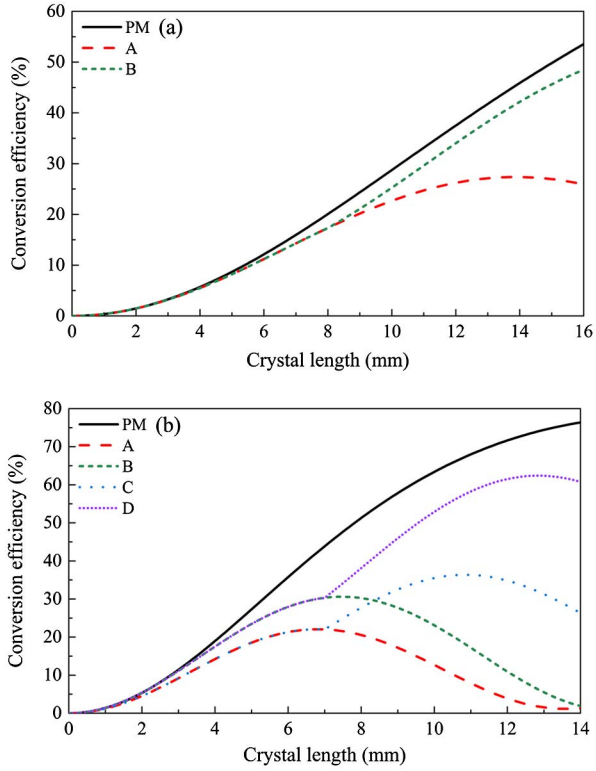

Fig. 7. Dependence of conversion efficiency on KDP crystal length for different conditions. (a) Frequency doubling by two 8 mm long KDP crystals in tandem. The solid line (line PM) indicates perfect phase matching; the dashed line (line A) indicates phase mismatch without compensation; the short-dashed line (line B) indicates that the phase mismatch is compensated. (b) Frequency tripling by two 7 mm long KDP crystals in tandem based on doubling. The solid line (line PM) indicates perfect phase matching for both doubling and tripling; the dashed line (line A) indicates both doubling and tripling phase mismatch without compensation; the short-dashed line (line B) indicates that only the doubling phase mismatch is compensated; the dotted line (line C) indicates that only the tripling phase mismatch is compensated; the short-dotted line (line D) indicates that both the doubling and tripling phase mismatch are compensated.

The conversion efficiencies of frequency doubling and tripling are approximately 53.6% and 76.4% at perfect phase-matching temperature, respectively, and are indicated by line PM in Figs. 7(a) and 7(b). The conversion efficiency will be reduced when the temperature deviates from the perfect phase-matching temperature. Comparing line A and line B in Fig. 7(a) shows that the output conversion efficiency of frequency doubling is obviously improved if the frequency doubling phase mismatch is compensated, and is similar in value to the conversion efficiency at the perfect phase-matching temperature (line PM).

For Fig. 7(b), line A is equivalent to frequency tripling using the traditional method with a single crystal. The conversion efficiency increases slowly and quickly reaches the point of maximum, and then begins to decrease so the final output efficiency is close to zero. The final efficiency of line B is almost zero because only the frequency doubling phase mismatch is compensated and the frequency tripling phase mismatch is not compensated, and thus the tripling conversion efficiency is almost unimproved. Line C in Fig. 7(b) shows that the output efficiency of tripling is improved when the frequency tripling phase mismatch is compensated. While the phase mismatch is compensated in the frequency doubling and tripling processes, it can be seen from line D in Fig. 7(b) that the output efficiency of tripling has been greatly improved.

As the crystal length affects both the efficiency and the temperature acceptance bandwidth of frequency conversion, the length of each single crystal in frequency doubling and tripling should be less than the coherence length (i.e., $L \le L_D = |\pi/\Delta k|$) in general [10]; otherwise, when the conversion efficiency reaches the extreme point, and the accumulated phase mismatch among the interacting waves is not yet compensated, the back-conversion process will occur rapidly and the conversion efficiency will start to decline. If the decreasing value of efficiency is very large, the conversion efficiency will not be improved significantly even if the phase mismatch is compensated, and hence the output efficiency will be low and the temperature acceptance bandwidth of frequency conversion will not be increased significantly. This is why it is difficult to obtain high conversion efficiency even with phase mismatch compensation when the temperature is changed by large amounts. Therefore, the length of the crystal is an important restraining factor in increasing the temperature acceptance bandwidth. In order to further increase the temperature acceptance bandwidth, a thin crystal and multiple phase mismatch compensation will be required.

In addition, the bandwidth of the fundamental wave also affects the conversion efficiency. For the frequency conversion by the traditional method, the bandwidth of the fundamental wave is limited by the nonlinear crystal. For our proposed method, the bandwidth of the fundamental wave is limited by the nonlinear crystal and the electro-optic crystal. But, the wavelength acceptance bandwidth of the electro-optic crystal can be increased by optimizing the length of the electro-optic crystal and voltage. The wavelength acceptance bandwidth is normally defined as the FWHM of the $\mathrm{sinc}^2[\Delta k(\lambda)L/2]$-function [31,32], where L is the length of the crystal. The wavelength acceptance bandwidths of DKDP crystal (the length is 20 mm and the voltage variation range is 0–10 kV)

for compensating frequency doubling and tripling phase mismatch are 1.066 and 0.664 nm, respectively. When a 5 mm length DKDP crystal is used with a voltage variation range of 0–40 kV, the corresponding wavelength acceptance bandwidths can reach 4.264 and 2.654 nm, respectively, which are much larger than the bandwidth of a high-power laser driver for ICF (~0.3 nm [2,33]).

D. Reflection Loss of Crystal Surface

For frequency doubling and tripling by the traditional method with a single crystal, each process only needs to pass through two surfaces (one crystal). However, each process has six surfaces (three crystals) if the phase mismatch is compensated by our proposed method. Therefore, it is necessary to analyze the reflection loss. According to [34], the coatings of crystals can reach a single-surface transmission of >99.5%. Thus, we assume that the single-surface transmission is 99.5%. The efficiencies of frequency doubling and tripling by the traditional method and our proposed compensation method (both the doubling and tripling phase mismatch are compensated) at 25°C, 26°C, and 28°C are shown in Table 2.

From Table 2, it can be seen that the output efficiencies of frequency doubling and tripling by our proposed scheme are 1.33% and 3.36% lower, respectively, than that of the traditional method at the phase-matching temperature (25°C).

However, the conversion efficiencies of frequency doubling and tripling using the traditional method are decreased by 3.85% and 21.04%, respectively, when the temperature is 26°C. The conversion efficiencies of frequency doubling and tripling are only decreased by 0.54% and 2.33%, respectively, when phase mismatch is compensated by our proposed method.

If the traditional method is used for frequency doubling and tripling, the conversion efficiencies will be reduced to 25.6% and 1.22%, respectively, when the temperature is 28°C. The efficiencies of frequency doubling and tripling using our proposed method still maintain high conversion efficiencies that can reach 46.66% and 56.72%, respectively.

Similar results can be obtained when the temperature is in the range of 22°C–25°C. According to the above analysis, we can conclude that our proposed method can effectively improve the efficiency of frequency conversion when temperature changes, although the conversion efficiency is decreased slightly at phase-matching temperature. Therefore, the influence of the reflection loss on the final output efficiency is very small.

Table 2. Efficiencies of Frequency Doubling and Tripling by Traditional Method and Our Proposed Compensation Method at 25°C, 26°C, and 28°C (Reflection Loss of Crystal Surfaces Is Considered)

Temperature	Scheme	Doubling (%)	Tripling (%)
PM (25°C)	Traditional	52.86	74.65
	Compensation	51.53	71.29
26°C	Traditional	49.01	53.61
	Compensation	50.99	69.57
28°C	Traditional	25.60	1.22
	Compensation	46.66	56.72

4. DISCUSSION

In this paper, the initial perfect phase-matching temperature for the KDP crystals is set at 25°C ($T_0 = 25$°C). In order to verify the effectiveness of our design method in improving the stability of the conversion efficiency, we assume that the temperature changes in the range of ±1°C. Then we randomly selected 192 temperatures between the range of 24°C–26°C to simulate the conversion efficiency of 192 laser beams in a practical application [2]. The corresponding conversion efficiencies of frequency doubling and tripling are shown in Fig. 8.

It can be seen from Fig. 8(a) that the distribution of frequency doubling conversion efficiency (beam to beam) is significantly improved by phase mismatch compensation, where lines A and B correspond to the standard deviations of 1.25% and 0.18%, respectively. For frequency tripling, as the temperature is randomly selected from the range between 24°C–26°C, and the differences between lines A and B in Fig. 5(b) are very small, the key to improving the frequency tripling conversion efficiency is to compensate for the tripling phase mismatch within this temperature range. Therefore, we compared the distribution of the frequency tripling conversion efficiency among the beams in the case of a traditional single crystal with our

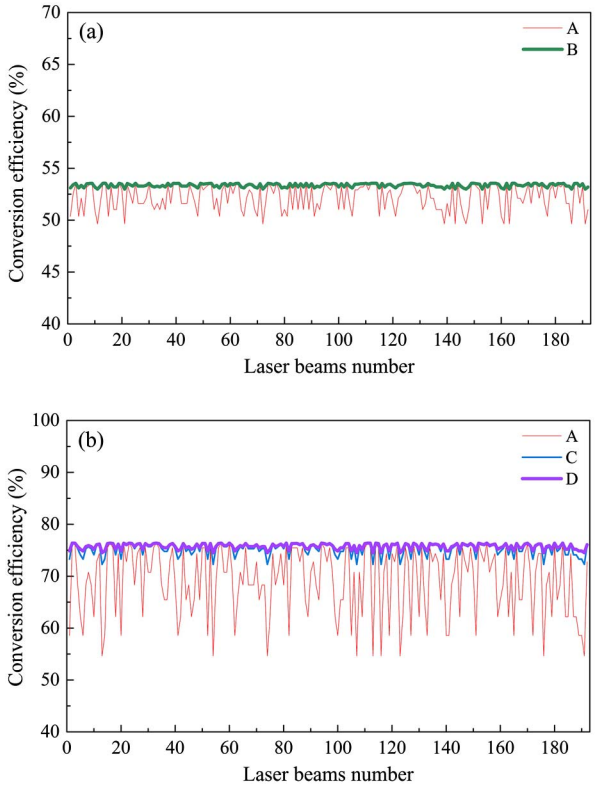

Fig. 8. Conversion efficiencies of 192 beams when temperature is randomly varied between the range of 24°C–26°C. (a) Frequency doubling, where the thin solid line (line A) indicates phase mismatch without compensation; the thick solid line (line B) indicates the phase mismatch is compensated. (b) Frequency tripling, where the thin solid line (line A) indicates both doubling and tripling phase mismatch without compensation; the thick solid line (line C) indicates that only the tripling phase mismatch is compensated; the most thick solid line (line D) indicates that both the doubling and tripling phase mismatch are compensated.

proposed design scheme, and the results are shown in Fig. 8(b). We can see that the change in the frequency tripling conversion efficiency by the traditional method is very severe [as shown by line A in Fig. 8(b)], and the standard deviation is 6.61%. The standard deviation is reduced to 1.19% when the frequency tripling phase mismatch is compensated. If both the frequency doubling and tripling phase mismatch are compensated, the standard deviation can be reduced to 0.56% and the maximum variation of output efficiency of frequency tripling is only 2.33% even though the reflection loss is considered (as shown in Table 2). Therefore, the energy and power among the beams can be well balanced.

According to the above discussion, it is clearly demonstrated that the fluctuation of temperature in a small range will have a great effect on the balance of efficiency among the beams [as shown by line A in Figs. 8(a) and 8(b)]. Compared with frequency doubling, the effect of this method for frequency tripling is more obvious. The phase mismatch can be well compensated by changing the voltage when temperature changes. The sensitivity of frequency doubling and tripling efficiency to temperature variation can be effectively reduced and the balance and stability of energy among output beams can be substantially improved. This may be an effective way to increase the temperature acceptance bandwidth of the frequency conversion in high-power laser systems, especially in the application of balance of energy and power for large laser facilities.

5. CONCLUSION

In conclusion, we proposed a novel scheme for phase mismatch compensation that can improve the temperature acceptance bandwidth of frequency conversion for high-power lasers. Further, the theoretical model of phase mismatch compensation by the electro-optic effect was established. Two nonlinear crystals and an electro-optic crystal were employed in this design, and it was found that the phase mismatch accumulated within the first crystal can be compensated in the electro-optic crystal. Adjustment of the voltage applied to the electro-optic crystal can achieve the phase mismatch compensation when the temperature is changed. Thus, a new dimension adjustment is added, and the stability of the conversion efficiency and the temperature acceptance bandwidth are substantially improved.

We present typical frequency doubling and tripling examples at a wavelength of 1053 nm. Numerical results show that the temperature acceptance bandwidth of frequency doubling and tripling is 2.4 and 3.4 times larger than that of a traditional single crystal, respectively, under a high-power regime. When the standard deviations of the conversion efficiencies of 192 beams were compared under different conditions, it was found that the stability of the conversion efficiency is significantly improved by our proposed phase mismatch compensation scheme. In addition, we also analyze the influence of the reflection loss on the final output efficiency. The results show that the reflection loss has little effect on the conversion efficiency. More importantly, this method is almost unlimited by the type of nonlinear crystals used, and the compensation for the phase mismatch can be achieved as long as the wavelengths of the laser beams are in the transmission range of the electro-optic crystal. Therefore, this scheme is not only able to compensate for the phase mismatch of the sum- and difference-frequency generations at various wavelengths, but also can compensate for the phase mismatch for different nonlinear crystals. This design provides a promising solution to the issue of temperature variation during the frequency conversion process and ensures the stability of energy and power of output beams, which will be especially useful in large laser facilities.

Funding. National Natural Science Foundation of China (NSFC) (11204327, 11304332)

REFERENCES

1. Y. Q. Liu, F. P. Yu, Z. P. Wang, S. Hou, L. Yang, X. G. Xu, and X. Zhao, "Bulk growth and nonlinear optical properties of thulium calcium oxyborate single crystals," CrystEngComm **16**, 7141–7148 (2014).
2. C. A. Haynam, P. J. Wegner, J. M. Auerbach, M. W. Bowers, S. N. Dixit, G. V. Erbert, G. M. Heestand, M. A. Henesian, M. R. Hermann, K. S. Jancaitis, K. R. Manes, C. D. Marshall, N. C. Mehta, J. Menapace, E. Moses, J. R. Murray, M. C. Nostrand, C. D. Orth, R. Patterson, R. A. Sacks, M. J. Shaw, M. Spaeth, S. B. Sutton, W. H. Williams, C. C. Widmayer, R. K. White, S. T. Yang, and B. M. Van Wonterghem, "National Ignition Facility laser performance status," Appl. Opt. **46**, 3276–3303 (2007).
3. L. L. Ji, B. Q. Zhu, C. Liu, T. Wang, and Z. Q. Lin, "Optimization of quadrature frequency conversion with type-II KDP for second harmonic generation of the nanosecond chirp pulse at 1053 nm," Chin. Opt. Lett. **12**, 031902 (2014).
4. R. C. Eckardt and J. Reintjes, "Phase matching limitations of high efficiency second harmonic generation," IEEE J. Quantum Electron. **20**, 1178–1187 (1984).
5. M. Webb, "Temperature sensitivity of KDP for phase-matched frequency conversion of 1 μm laser light," IEEE J. Quantum Electron. **30**, 1934–1942 (1994).
6. F. Raoult, A. C. L. Boscheron, D. Husson, C. Rouyer, C. Sauteret, and A. Migus, "Ultrashort, intense ultraviolet pulse generation by efficient frequency tripling and adapted phase matching," Opt. Lett. **24**, 354–356 (1999).
7. M. Shaw, W. Williams, R. House, and C. Haynam, "Laser performance operations model," Opt. Eng. **43**, 2885–2895 (2004).
8. Y. C. Liang, R. F. Su, L. H. Lu, and H. T. Liu, "Temperature nonuniformity occurring during the cooling process of a KDP crystal and its effects on second harmonic generation," Appl. Opt. **53**, 5109–5116 (2014).
9. D. T. Hon and H. Bruesselabach, "Beam shaping to suppress phase mismatch in high power second-harmonic generation," IEEE J. Quantum Electron. **16**, 1356–1364 (1980).
10. H. Z. Zhong, P. Yuan, and H. Y. Zhu, and L. J. Qian, "Versatile temperature-insensitive second-harmonic generation by compensating thermally induced phase-mismatch in a two-crystal design," Laser Phys. Lett. **9**, 434–439 (2012).
11. H. Z. Zhong, P. Yuan, S. C. Wen, and L. J. Qian, "Temperature-insensitive frequency tripling for generating high-average power UV lasers," Opt. Express **22**, 4267–4276 (2014).
12. L. L. Wang, Y. Chen, and G. C. Liu, "Increased temperature acceptance bandwidth in frequency-doubling process using two different crystals," Chin. Opt. Lett. **12**, 111902 (2014).
13. A. H. Wu, J. Xu, Y. Q. Zheng, and X. Y. Liang, "Crystal growth and application of large size YCOB crystal for high power laser," Opt. Mater. **36**, 2000–2003 (2014).
14. Z. G. Hu, Y. Zhao, Y. C. Yue, and X. S. Yu, "Large LBO crystal growth at 2kg-level," J. Cryst. Growth **335**, 133–137 (2011).
15. A. Yariv and P. Yeh, *Optical Waves in Crystals* (Wiley, 1984).
16. B. A. Liu, G. H. Hu, Q. H. Zhang, X. Sun, and X. G. Xu, "Effect of raw material and growth method on optical properties of DKDP crystal," Chin. Opt. Lett. **12**, 101604 (2014).

17. S. T. Yang, M. A. Henesian, T. L. Weiland, J. L. Vickers, R. L. Luthi, J. P. Bielecki, and P. J. Wegner, "Noncritically phase-matched fourth harmonic generation of Nd:glass lasers in partially deuterated KDP crystals," Opt. Lett. **36**, 1824–1826 (2011).
18. D. N. Nikogosyan, *Nonlinear Optical Crystals: A Complete Survey* (Springer, 2005).
19. A. Yariv and P. Yeh, *Photonics: Optical Electronics in Modern Communications*, 6th ed. (Oxford University, 2007).
20. G. C. Ghosh and G. C. Bhar, "Temperature dispersion in ADP, KDP, and KD* P for nonlinear devices," IEEE J. Quantum Electron. **18**, 143–145 (1982).
21. W. Wang, W. Han, F. Wang, J. Wang, L. D. Zhou, H. T. Jia, Y. Xiang, K. Y. Li, F. Q. Li, L. Q. Wang, W. Zhong, X. M. Zhang, S. Z. Zhao, and B. Feng, "Comparison of efficient third-harmonic generation between phase modulated broadband and narrowband lasers," J. Opt. Soc. Am. B **28**, 475–482 (2011).
22. A. V. Smith, D. J. Armstrong, and W. J. Alford, "Increased acceptance bandwidths in optical frequency conversion by use of multiple walk-off-compensating nonlinear crystals," J. Opt. Soc. Am. B **15**, 122–141 (1998).
23. K. Li and B. Zhang, "Analysis of broadband third harmonic generation with non-collinear angular dispersion in KDP crystals," Opt. Commun. **281**, 2271–2278 (2008).
24. D. Eimerl, J. M. Auerbach, and W. Milonni, "Paraxial wave theory of second and third harmonic generation in uniaxial crystals: I. Narrowband pump fields," J. Mod. Opt. **42**, 1037–1067 (1995).
25. M. Born and E. Wolf, *Principles of Optics*, 7th ed. (Cambridge University, 1999).
26. M. Aoyama, T. Harimoto, J. Ma, Y. Akahane, and K. Yamakawa, "Second-harmonic generation of ultra-high intensity femtosecond pulses with a KDP crystal," Opt. Express **9**, 579–585 (2001).
27. P. Banks, M. Feit, and M. Perry, "High-intensity third-harmonic generation," J. Opt. Soc. Am. B **19**, 102–118 (2002).
28. A. J. Taylor, G. Rodriguez, and T. S. Clement, "Determination of n_2 by direct measurement of the optical phase," Opt. Lett. **21**, 1812–1814 (1996).
29. K. M. Guo, J. Q. Lin, Z. Q. Hao, X. Gao, Z. M. Zhao, C. K. Sun, and B. Z. Li, "Triggering and guiding high-voltage discharge in air by single and multiple femtosecond filaments," Opt. Lett. **37**, 259–261 (2012).
30. M. Henriksson, J.-F. Daigle, F. Théberge, M. Châteauneuf, and J. Dubois, "Laser guiding of Tesla coil high voltage discharges," Opt. Express **20**, 12721–12728 (2012).
31. T. Kellner, F. Heine, and G. Huber, "Efficient laser performance of Nd: YAG and intracavity frequency doubling with LiJO3, β–BaB2O4, and LiB3O5," Appl. Phys. B **65**, 789–792 (1997).
32. Z. Cao, X. Gao, W. Chen, H. Wang, W. Zhang, and Z. Gong, "Study of quasi-phase matching wavelength acceptance bandwidth for periodically poled $LiNbO_3$ crystal-based difference-frequency generation," Opt. Lasers Eng. **47**, 589–593 (2009).
33. X. W. Deng, F. Wang, H. T. Jia, Y. Xiang Yong, B. Feng, K. Y. Li, and L. D. Zhou, "Temporal, spectral and spatial characterization of high-energy laser pulse with small bandwidth propagating through long path," Chin. Phys. Lett. **29**, 124211 (2012).
34. J. H. Campbell, R. A. Hawley-Fedder, C. J. Stolz, J. A. Menapace, M. R. Borden, P. K. Whitman, J. Yu, M. Runkel, M. O. Riley, M. D. Feit, and R. P. Hackel, "NIF optical materials and fabrication technologies: an overview," Proc. SPIE **5341**, 84–101 (2004).